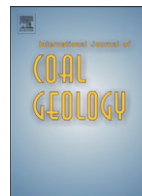




Contents lists available at ScienceDirect

## International Journal of Coal Geology

journal homepage: [www.elsevier.com/locate/ijcoalgeo](http://www.elsevier.com/locate/ijcoalgeo)

# The origin and formation of CO<sub>2</sub> gas pools in the coal seam of the Yaojie coalfield in China

Wei Li, Yuan-Ping Cheng\*, Lei Wang

National Engineering Research Center for Coal &amp; Gas Control, China University of Mining &amp; Technology, Xuzhou 221008, China

## ARTICLE INFO

## Article history:

Received 23 July 2010

Received in revised form 16 November 2010

Accepted 16 November 2010

Available online xxxx

## Keywords:

Carbon dioxide

Carbon isotope

Dynamic metamorphism

Yaojie coalfield

F19 fault

## ABSTRACT

High concentrations of CO<sub>2</sub> have been observed in the No. 2 coal seam in the Yaojie coalfield. A number of instantaneous CO<sub>2</sub> outbursts occurred during coal mining. The CO<sub>2</sub> concentration range in the eastern coalfield is 18.79 to 96.6%. The  $\delta^{13}\text{C}_{\text{CO}_2}$  values are mainly in the range of  $-5.0\text{‰}$  to  $+1.0\text{‰}$  (PDB), suggesting an inorganic origin of CO<sub>2</sub>. The  $^3\text{He}/^4\text{He}$  ratios are  $(0.6\text{--}25.9) \times 10^{-8}$ , and the  $R/R_a$  is 0.0042–0.185, which is a characteristic of crust-derived CO<sub>2</sub> gas. The dynamic-thermal metamorphism of the F19 ductile-brittle shear zone is believed to result in the release of CO<sub>2</sub> from basement marble formations, which show an inorganic source of CO<sub>2</sub> in the Yaojie coalfield. The regional geological evolution and multi-periodical F19 fault movement control the formation, migration, and accumulation of the CO<sub>2</sub>, in addition to the development of CO<sub>2</sub> gas pools in the Yaojie coalfield. The F19 fault played multiple roles in the generation, transport, and sequestration of gas during the CO<sub>2</sub> formation. The displacement of CH<sub>4</sub>, carbonate generation, and pore structure transformation of coal due to a series of physical and chemical effects occurred after CO<sub>2</sub> flux into the coal seams.

© 2010 Published by Elsevier B.V.

## 1. Introduction

The No. 2 coal seam in the Yaojie coalfield, located in northwestern China, is characterized by extensive CO<sub>2</sub> distributions. A number of instantaneous CO<sub>2</sub> outbursts have occurred during coal mining since 1977. There are various potential sources of CO<sub>2</sub> in the Yaojie Coalfield, such as magmatic origin, mantle degassing, and the spontaneous combustion of coal (Tao, 1993; Wei et al., 2007). Locations that are associated with rock and CO<sub>2</sub> outbursts include the Yanbian and Helong Mines in China (Yu, 1992), the Cevennes Basin in France, the Lower Silesia in Poland, and the Sydney and Bowen Basins in Australia (Lama and Bodziony, 1998; Beamish and Crosdale, 1998; Faiz et al., 2007). While volcanic and magma activities are the typical sources of CO<sub>2</sub> outbursts, CO<sub>2</sub> penetrates the coal seams through deep faults and attenuated coal formation. However, few studies have been conducted on CO<sub>2</sub> migration and accumulation in coal strata.

The volcanic or geothermal areas and the magma degassing or thermo-metamorphic alteration of carbonates result in the production of large amounts of CO<sub>2</sub> (Clayton, 1998; Pearce et al., 2004; Annunziatellis et al., 2008). Fault zones can act as barriers, conduits, or mixed conduit-barrier systems. Deep faults in the reservoir play an important role in the process of CO<sub>2</sub> accumulation, which is controlled by regional tectonic movements in the forms of generation, migration,

accumulation or dispersion and preservation (Antonellini et al., 1994; Evans et al., 1997; Sibson, 2000).

In this study, CO<sub>2</sub> concentrations coupled to carbon and helium isotopes are analyzed to evaluate the origins of CO<sub>2</sub> in the Yaojie coal seam. The large-scale regional tectonic features and evolutionary activities of the F19 fault are also employed in the derivations. Migration and accumulation processes are analyzed based on a geological survey of CO<sub>2</sub> characteristics in the coal seam. The research presented in this work can unveil occurrence CO<sub>2</sub> in the coal seam, based on which some precautionary steps can be taken on CO<sub>2</sub> drainage to prevent and treat the coal and CO<sub>2</sub> outburst. These results also may provide a natural analog for assessing the deep storage of CO<sub>2</sub> in coal seams.

## 2. Regional geological evolutions

The Yaojie coalfield is located in the western margin of Minhe and extends across the Gansu and Qinghai provinces, consisting of the Yaojie No. III mine and Haishiwan coalfield (shown in Fig. 1). The Minhe basin is a mountain depression basin that developed during the Mesozoic–Cenozoic on the Qilian orogenic belt. The current structural layer of the basement lies mainly in the NW direction. The main source of significant deformation occurred in the early Yanshan tectonic (208–135 Ma) when the primary tectonic stress was in the NE direction. The primary regional tectonic compression stress of the middle and late Yanshan tectonic (135–65 Ma) was primarily in the NW–NNE direction. The principal compression stress of the Himalayan tectonic (23.5–0.78 Ma) was in the NW direction. The analysis above

\* Corresponding author. Tel.: +86 516 83885948; fax: +86 516 83995097.  
E-mail addresses: [liwei5005@126.com](mailto:liwei5005@126.com), [ypc620924@163.com](mailto:ypc620924@163.com) (Y.-P. Cheng).

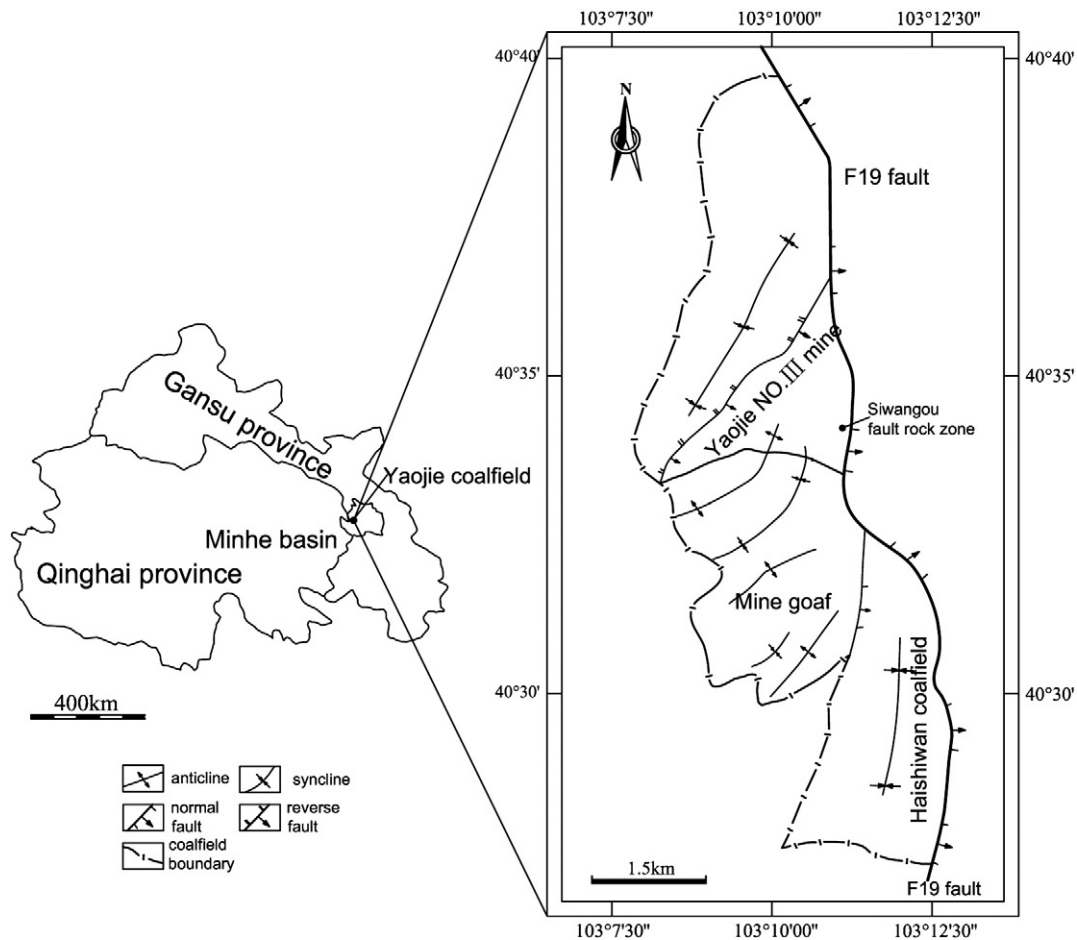


Fig. 1. Map showing the study area and data locations for gas volume, composition, and geochemical characteristics.

indicates that the structure is well developed with multiple stages and tectonic movements (Cao, 1997; Zhao et al., 2000). The current principal compression stress of the tectonic stress field is in the NE direction. The basin stratum is Mesozoic–Cenozoic sedimentary, which generally lacks Paleozoic and Mesozoic sedimentary Triassic deposits, and the basement is Proterozoic metamorphic sedimentary (Tao et al., 1995).

The Proterozoic basement mainly composes of marble, gneiss, quartz schist, and siliceous limestone, making up a cluster of metamorphic rocks with a thickness greater than 6000 m and outcropped in surrounding of Yaojie coalfield (Wei et al., 2007). The coal-bearing strata of the Yaojie coalfield is part of the Yaojie series in the Jurassic system middle stratium. The Yaojie coalfield lies roughly on a NNW direction with the F19 fault zone located to the east of it. The coal basin is directly integrated at the top of the Huangyuan Group. The total average thickness is 163 m with the coal seam at approximately 30 m. Coal seams are located primarily in the lower second petrofabric. Two of the three coal seams are suitable for mining. The No. 2 coal seam is a primary coal bed suitable for mining with hazards of coal and CO<sub>2</sub> outbursts (Fig. 2). The No. 1 coal seam, the other minable coal seam, produces sapropelic coal with maximum vitrinite reflectance (VR) values ranging from approximately 0.511 to 0.584%. Coal from the No. 2 coal seam is high volatile bituminous with maximum vitrinite reflectance (VR) values ranging from approximately 0.690 to 1.056%.

### 3. Materials and methods

The current study was conducted by compiling information from published and unpublished data on exploration boreholes and

underground coal mines. This information has been supplemented with new data obtained from the sample measurements of selected locations.

The carbon isotopic composition of gas was determined on a DeltaPlusXP isotopic mass spectrometer equipped with an Agilent 5890 NGC at the Lanzhou Institute of Geology of the Chinese Academy of Science. Hydrocarbon gas compounds were separated individually using a capillary column (30 m × 0.32 mm × 0.53 mm C2000). The inlet temperature was 30 °C, the oxidation oven temperature was 840°, and the gas chromatograph temperature began at 30 °C for 5 min followed by an increase from 30 °C to 200 °C at a rate of 15 °C/min. The analytical precisions for the measured  $\delta^{13}\text{C}_{\text{CO}_2}$  values for CO<sub>2</sub> are within ± 0.02‰ based on the PDB standard.

The helium isotope compositions were performed using a noble gas mass spectrometer (VG5400 VG Isotopes) at the Lanzhou Institute of Geology of the Chinese Academy of Science. An inlet system with high vacuum purification line, low leakage, and low background levels was used. Based on multiple analyses on laboratory standards, reproducibility of  $^3\text{He}/^4\text{He}$  measurements are better than ± 2%.

The detailed analytical conditions are described by Ye et al. (2001, 2007).

The maceral group composition and minerals was determined using a reflection polarizing microscope (DTACX-P01) at the Institute of Coalfield Geology of the Gansu Coal Geological Bureau. Through bonding, molding, and polishing, the air-dried coal samples with particle sizes less than 1 mm were obtained in polished sections. The polished section of powder coal was visualized underneath the reflection of a polarizing microscope with white incident light. With a cross polarizer or monopolarizer and clear identification, the maceral group composition and minerals were determined using a point

Erathem	System	Series	Group	Formation	Thickness (m)	Lithological succession	Lithology description	
Cenozoic	Quaternary	upper		Q <sub>3m</sub>	0-236.34		Loess	
		Mid		Q <sub>21</sub>	0-24.07		Gravel	
Mesozoic	Cretaceous		Minhe	K <sub>2mh</sub>	28.18-369.2		Glutenite	
		Lower	Hekou	K <sub>1hk</sub> <sup>7</sup>	50.66-408.3		Mudstone Glutenite	
				K <sub>1hk</sub> <sup>6</sup>	162.33-518.07		Sandy Mudstone	
				K <sub>1hk</sub> <sup>4</sup>	33.13-414.50		Mudstone Sandy Mudstone	
		Jurassic	upper	Xiangtang	J <sub>2xt</sub> <sup>3</sup>	24.25-261.79		Mudstone Silt-finestone
					J <sub>2xt</sub> <sup>2</sup>	26.19-158.68		Mudstone Fine sandstone Medium sandstone
	J <sub>2xt</sub> <sup>1</sup>				17.17-134.52		Sandy Mudstone Sandstone Conglomerate	
	Mid		Yaojie	J <sub>2yj</sub> <sup>5</sup>	12.09-73.79		Mudstone medium-sandstone fine sandstone	
				J <sub>2yj</sub> <sup>4</sup>	6.71-94.20		Oil shale Sand shale Reservoir sandstone	
				J <sub>2yj</sub> <sup>3</sup>	0.32-14.73		Marlite NO.1 coal seam Oil shale	
				J <sub>2yj</sub> <sup>2</sup>	0-110.3		Carbonaceous rock Siltite NO.2 coal seam Carbonaceous rock NO.3 coal seam	
	J <sub>2yj</sub> <sup>1</sup>	0-22.38		Conglomerate Silt-finestone				
	Lower	Tandonggou	J <sub>1td</sub>	0-310.34		Conglomerate Glutenite		
Proterozoic			Pt	unkown		Marble Gneiss Quartz schist Siliceous limestone		

Fig. 2. Generalized stratigraphy and tectonic events of the Yaojie coalfield.

counting method. The detailed experimental procedure was performed according to the requirements of the National Standards of the People's Republic of China (GB/T 8899-1998, GB/T16733-1997).

Coalbed gas content were determined using the desorption method during the geological exploration in accordance with the China Safety Industry Standards (AQ1066-2008; MT/T77-1994). In situ gas contents were determined according to the formula (1):

$$X_0 = \frac{V_1 + V_2 + V_3 + V_4}{Q} \quad (1)$$

where  $X_0$  is the total in situ gas contents (ml/g),  $V_1$  is the desorption gas content in the mine (ml),  $V_2$  is the gas loss content (ml),  $V_3$  is the

negative pressure desorption gas content before comminution (ml),  $V_4$  is the negative pressure desorption gas content during comminution (ml), and  $Q$  is the coal sample quality (g).  $V_2$  was obtained from the empirical formula, while  $V_3$  and  $V_4$  were determined in the laboratory. Gas volume was converted to standard conditions (0 °C, 101.3 kPa).

#### 4. Results and discussions

##### 4.1. Geochemical characteristics of natural gas

The molecular composition of  $CO_2$  from the Yaojie coalfield is determined from gas samples of the geological surface and mine borehole of the No. 2 coal seam, as shown in Table 1 (data from Tao

**Table 1**  
Composition and geochemical characteristics of CO<sub>2</sub> in the eastern Yaojie coalfield (data from Tao et al., 1991; Tao, 1993 and new experimental determination).

Region	CO <sub>2</sub> (%)	δ <sup>13</sup> C <sub>CO<sub>2</sub></sub> (‰, PDB)	<sup>3</sup> He/ <sup>4</sup> He (×10 <sup>-8</sup> )	R/Ra	δ <sup>18</sup> O <sub>CO<sub>2</sub></sub> (‰, SMOW)	Data sources
Haishiwan coalfield	84.39	-3.6	20.3	0.1450	23.43	This paper
	81.53	-4.6	5.07	0.0362		
	89.65	-0.35				
	74.25	-3.66			21.93	
	76.62	-4.11			22.23	
	58.85	-3.79			21.81	
	18.79	-4.79				
	68.82	+1.12				
	96.20	-4.94			19.88	
	85.07	-1.27	3.92	0.0280	24.22	
89.39	-1.38	3.49	0.0250	24.07		
89.30	-9.41			18.65		
89.67	-9.94			16.29		
88.32	-8.00					
Yaojie NO. III coal mine	95.40	-0.55	10.1	0.0720	22.17	Tao, 1991; Tao, 1993
	96.60	-4.06	25.9	0.1850	19.89	
	96.60	-4.64	3.8	0.0270	20.47	
	88.10	-2.98	0.6	0.0042	20.78	
	87.38	-3.65	2.2	0.0150	21.90	

et al., 1991; Tao, 1993 and new experimental determination). The CO<sub>2</sub> concentration ranges from 18.79 to 96.60% of the total gas content with an average of 81.83% in the eastern coalfield. Other species are methane, nitrogen, and hydrocarbon. The highest CO<sub>2</sub> contents are distributed in the eastern Yaojie coalfield. According to the literature, the CO<sub>2</sub> is inorganic if the CO<sub>2</sub> composition accounts for more than 60% in gas pools. Therefore, CO<sub>2</sub> derived from coal spontaneous combustion is excluded.

The measured δ<sup>13</sup>C<sub>CO<sub>2</sub></sub> values range from +1.12‰ and -20.00‰ (Fig. 3; Table 3), and most of them are in the range of -5.0‰ to +1.0‰. <sup>3</sup>He/<sup>4</sup>He values ranges from (0.6 ± 0.6) × 10<sup>-8</sup> to (25.9 ± 0.3) × 10<sup>-8</sup>, and R/Ra value ranges from 0.0042 to 0.185 (where Ra is the atmospheric value of <sup>3</sup>He/<sup>4</sup>He and R the sample value of <sup>3</sup>He/<sup>4</sup>He). These results indicate that He is derived from the crust and implies that CO<sub>2</sub> in the Yaojie coalfield is of crustal origin. The δ<sup>13</sup>C<sub>CH<sub>4</sub></sub> of the No. 2 coal seam gas ranges from -32.76‰ to -44.08‰ (Wei et al., 2007), indicating that the methane is of organic origin and not related to inorganic CO<sub>2</sub>.

The present CO<sub>2</sub> in coalbeds can be the result from several processes that are not related to coalification, including recent

microbiological activities, the thermal degradation of carbonates, and the migration from magma chambers or the upper mantle (Smith and Pallasser, 1996; Clayton, 1998). The δ<sup>13</sup>C values of metamorphic CO<sub>2</sub> derived from carbonate thermal decomposition are close to the mean δ<sup>13</sup>C values of carbonate rocks (0 ± 3‰). CO<sub>2</sub> with δ<sup>13</sup>C<sub>CO<sub>2</sub></sub> values in the range of -4‰ to -7‰ is considered mantle-derived. (Clayton et al., 1990; Thrasher and Fleet, 1995). Carbon isotopic fractionation and organogenic CO<sub>2</sub> mixes result in reduced δ<sup>13</sup>C values of CO<sub>2</sub> from decarbonization. There is a significantly positive correlation between CO<sub>2</sub> contents and δ<sup>13</sup>C<sub>CO<sub>2</sub></sub> values of CO<sub>2</sub> from the Yaojie coalfield (Fig. 3).

Tao (1993) measured the δ<sup>13</sup>C and δ<sup>18</sup>O of calcite veins and CO<sub>2</sub> from the No. 2 coal seam and the Yaojie coalfield roof and floor. Most δ<sup>13</sup>C and δ<sup>18</sup>O values for CO<sub>2</sub> and calcite do not fall within the interval of carbonate (Fig. 4). The O and C isotope interaction between calcite and fluid primarily reflects the calcite-water fractionation and calcite - H<sub>2</sub>CO<sub>3</sub> or HCO<sub>3</sub><sup>-</sup> fractionation, respectively. The C and O isotope of calcite tends to display much smaller variation in the δ<sup>13</sup>C values than the δ<sup>18</sup>O values due to the precipitation of calcite in a HCO<sub>3</sub><sup>-</sup> dominant fluid. A positive correlation between δ<sup>13</sup>C and δ<sup>18</sup>O values for CO<sub>2</sub> may be due to a progressive decrease in temperature during CO<sub>2</sub> degassing (Zheng, 1990). The dissolving and degassing of CO<sub>2</sub> accompanied by the C and O isotope fractionation generates the trace calcite veins of the Yaojie coalfield. Moreover, the isotope fractionation of multi-source CO<sub>2</sub> occurs because of the co-existence of inorganic and organic CO<sub>2</sub> in the coal seam. When different isotopic composition of CO<sub>2</sub> are mixed, their equilibrium conditions depend on the chemical and physical conditions in the process, e.g. temperature, adsorption/desorption process (Valkiers et al., 2007).

#### 4.2. Crustal sources of CO<sub>2</sub>

Crustal sources of CO<sub>2</sub> can be divided into contact metamorphism of carbonates and dynamic metamorphism of fault activities. The pyroxenite, serpentized peridotite, and serpentinite form a basic-ultrabasic rock band that is distributed along the F19 fault discontinuously. The amphibole isotopic age (K-Ar method) is 323–366 Ma, and the geological age of Hercynian magmatic activities is earlier than that for Jurassic coal (Wei et al., 2007). No magmatic activities have occurred in the region since the Paleozoic (Gansu Province Geology and Mining Bureau, 1989; Tao, 1993). Magmatic rock was not found during the geological exploration of the Haishiwan coalfield. Therefore, there is little possibility that CO<sub>2</sub> is derived from contact metamorphism of carbonates.

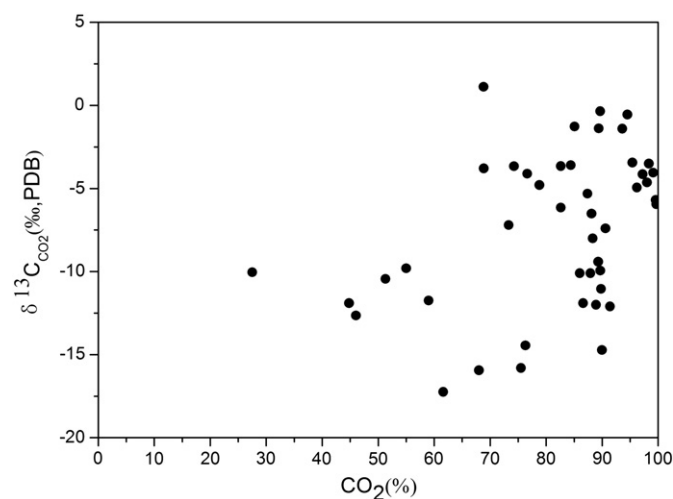


**Fig. 3.** CO<sub>2</sub> concentrations and δ<sup>13</sup>C<sub>CO<sub>2</sub></sub>(PDB) values for CO<sub>2</sub> from the No. 2 coal seam in the Yaojie coalfield.

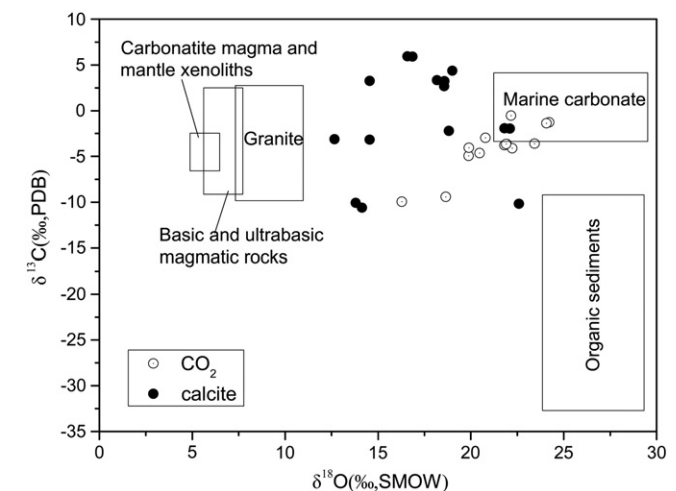


**Fig. 4.** Carbon and oxygen isotope compositions of CO<sub>2</sub> and calcite in the Yaojie coalfield (in ‰ relative to PDB and SMOW, respectively, and modified according to Liu et al., 1997).

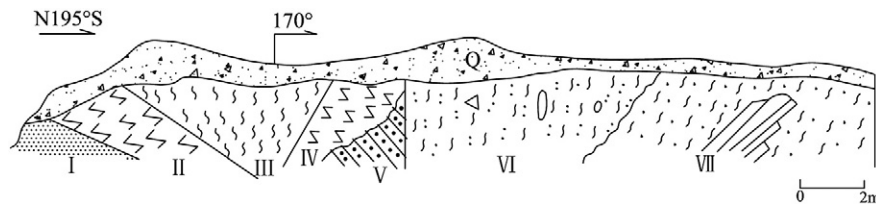


Fig. 5. Geological survey profile of the F19 fault belt tectonite in Siwangou, Q(Quaternary strata) (Tao et al., 1995).

Dynamic metamorphism is the only source of CO<sub>2</sub> in the Yaojie coalfield as determined by the exclusion approach. Proof of dynamic metamorphism is important to verify our hypotheses. The fracture zone of the F19 fault outcrops for 30 m in the southern foothills of Siwangou (Fig. 5). Many types of tectonic filling fault fracture zones with mixed characteristics have appeared featured with sequence in the cross-section and assembly characteristics of the tectonite belt, as shown in Table 2.

The altered rock belt is influenced by both fracture force and hydrothermal activities with diverse structural and tectonic features. The stress generation of minerals and dynamic metamorphism of the tectonic belt is obvious, e.g. epidote, cataclasite, wavy extinction, and crackle. Mylonite formed by extruded rub reflects typical ductile-brittle shearing. The process was accompanied by chloritization, strong silicification and calcite disappearance. These phenomena indicate strong structural-hydrothermal activities (Wang and Zhu, 1995; He et al., 1996). These activities of brittle-ductile shear zone result in the development of significant decarbonization of carbonatite, element differentiation, migration, and CO<sub>2</sub> formation in the fault zone (O'Hara and William, 1989; O'Hara, 1994). This is the main source of inorganic CO<sub>2</sub> formed with the dynamic metamorphism of the fault zone. The amount of CO<sub>2</sub> generated is closely related to fluid interaction, rheological behavior of rocks, and rock volume loss. Theoretical studies demonstrate that every 100 g of carbonate rock mass generates 22.90–33.90 g of CO<sub>2</sub> during the structural dynamic metamorphism (Tao et al., 2000; Yang et al., 1997, 2002). During the Yanshan movement and Himalayan movement from the late Jurassic to the early Neogene, the structural thermal-dynamic and action of the brittle-ductile shear zone of the F19 fault caused the marble at the basement to decompose into CO<sub>2</sub>.

Therefore, a general downwards progression in dominant fault-rocks (gouge–breccia–cataclasite–phylionite–mylonite–mylonitic gneiss) is inferred for a normal fault zone developed in the quartzofeldspathic crust, as shown in Fig. 6. The fault rock distribution of

Table 2

Features of tectonite divisions and fault rock distribution in the Siwangou geological survey profile.

Tectonite divisions	Rock belt names	Main mineral	Main features
I	Fault gouge	Sericite Chlorite plagioclase quartz	Polysynthetic twin developed
II	Mylonite	Quartz Epidote chlorite	Obvious plastic rheological phenomenon of rock
III	Cataclasite	Chlorite schist	Fragment rock and fractures filled with carbonatite dyke
IV	Sallow mylonite	Quartz	Polysynthetic twin developed
V	Cataclasite (sandstone)	Feldspar	Tartan twinning and polysynthetic twin developed; undulatory extinction
VI	Scaly mudstone hybrid zone	Calcite	Mudstones schistosity developed; calcites vein nearly vertically developed
VII	Cataclasite	Chlorite quartz Oil sands	Rock fragmentation with oil sand rock block

Siwangou horizontal zoning quarry suggests that ductile-brittle shear and fault rock zoning of the F19 fault occur in the vertical direction. Stable mineral assemblages of the F19 fault are quartz–feldspar–sericite–chlorite. Therefore, the isotherm defining the onset of stable mineral assemblage conditions is estimated in the range of 350–500 °C. For normal geothermal gradients of 30 °C/km, the 350–500 °C hydrotherm is within the 11–16 km interval. The estimated 11 km (350 °C) depth is the cataclasite–phylionite transition of the normal fault. In the regions deficient in water, the transition may occur at greater temperatures and depth (Sibson, 2000). Under water participation, the reactive dissolution of carbonatite could product large quantities of CO<sub>2</sub> at temperatures between 70 and 220 °C (Hutcheon et al., 1990).

#### 4.3. The characteristics of CO<sub>2</sub> transport in the No. 2 coal seam

Contents and gas compositions of CO<sub>2</sub> and CH<sub>4</sub> were determined from 27 surface borehole samples for the No. 2 coal seam of the Haishiwan coalfield (Fig. 7; Table 3). In situ CO<sub>2</sub> gas contents of coal in No. 2 ranges from 0.3 to 10 m<sup>3</sup>/t, and CH<sub>4</sub> gas contents ranges from 0.05 to 6.22 m<sup>3</sup>/t. Gas composition for CO<sub>2</sub> from coal seams of the No. 2 coal varies between 15.47% and 90.89% and between 0.48% and 68.79% for CH<sub>4</sub>.

The gas content and gas compositions of the samples are plotted against the distance from the F19 fault (Fig. 8). The CO<sub>2</sub> content decreases and the CH<sub>4</sub> content increases along the distance from the

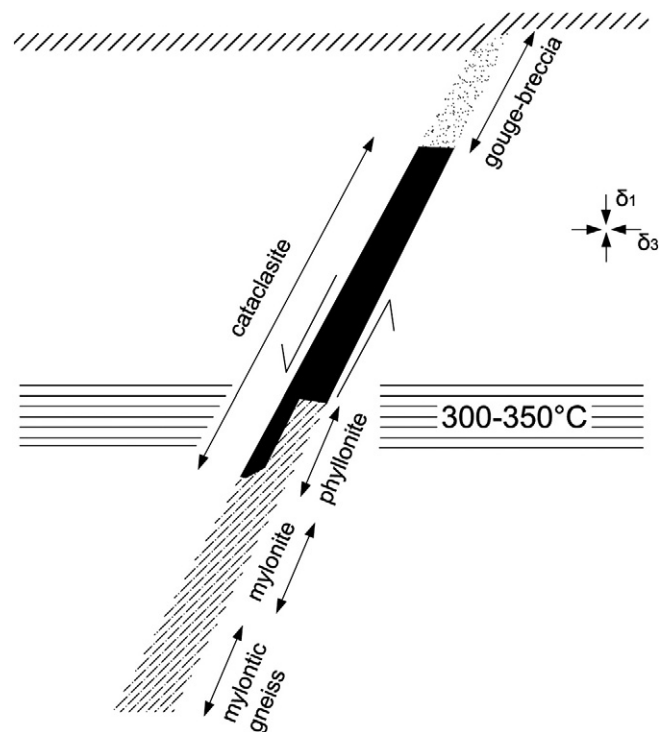


Fig. 6. The fault rock distribution for an optimally oriented crustal-scale normal fault (Sibson, 2000).

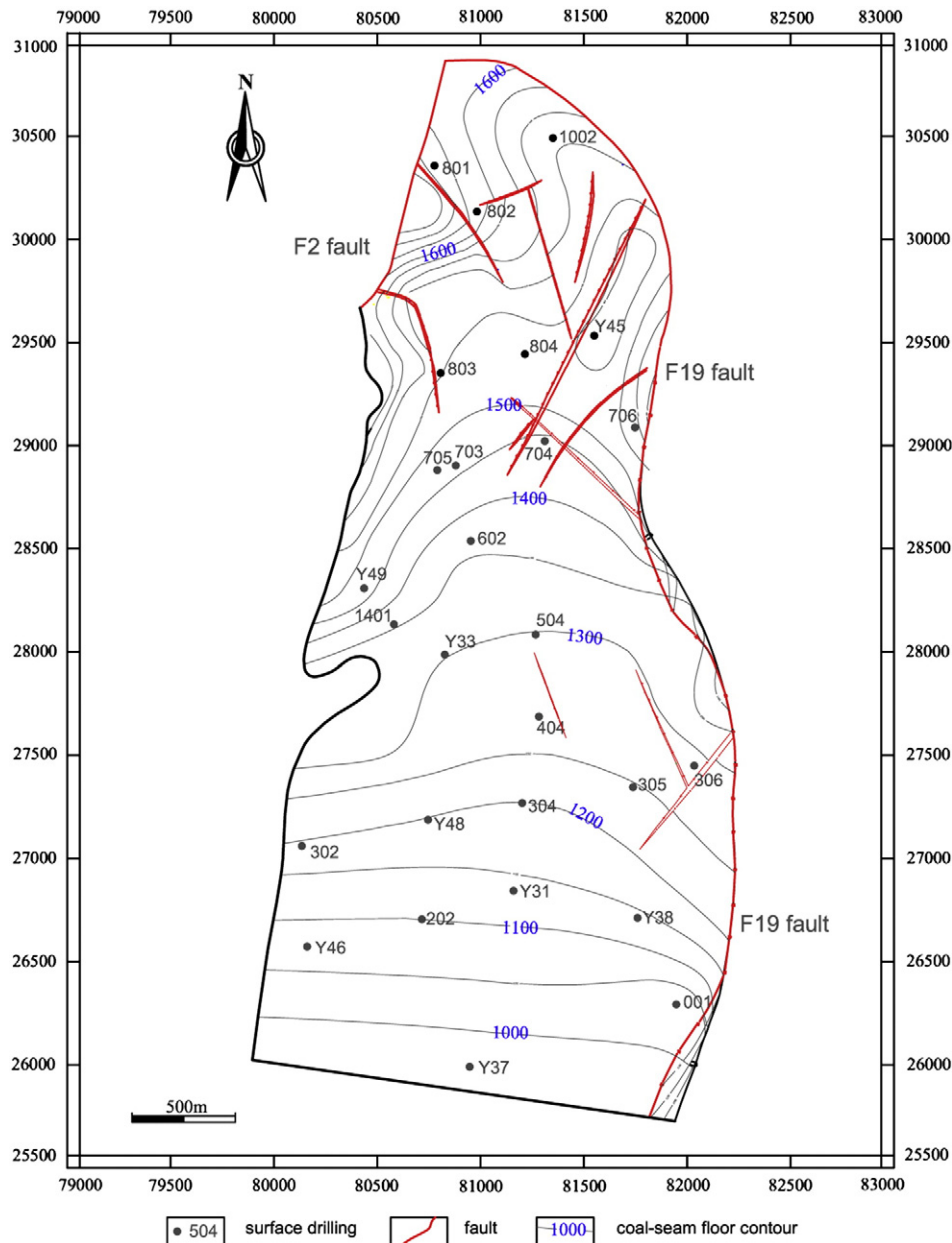


Fig. 7. Arrangement of exploration boreholes in the Haishiwan coalfield. The altitude of ground ranges from 1900 to 2300 m from the valley and mountain covering.

F19 fault. The  $\text{CO}_2$  and  $\text{CH}_4$  composition show the same trend as the distance from the F19 fault. The  $\text{CO}_2$  gas content does not change and the  $\text{CO}_2$  balance of the reservoir gas injection direction is related to change in this imbalance and preserves for a long period in geological history.

The identification of the general direction of  $\text{CO}_2$  migration also constrains the timing of the  $\text{CO}_2$  input relative to  $\text{CH}_4$ . Assumed by simple filling, the samples closest to the  $\text{CO}_2$  source might be expected to have the highest  $\text{CO}_2$  concentrations and contents after  $\text{CH}_4$  production (Ballentine et al., 2000).  $\text{CO}_2$  can be sequestered into coal seams while  $\text{CH}_4$  is recovered from the depleted coal seams by  $\text{CO}_2$  injection. The distribution of  $\text{CO}_2$  and  $\text{CH}_4$  is consistent with an initial input of  $\text{CO}_2$  from the east of the F19 fault with subsequent  $\text{CH}_4$  generation in the No. 2 coal seam.

The  $\delta^{13}\text{C}_{\text{CO}_2}$  values ( $-20.0\%$  to  $-0.35\%$ ) vary with increasing distance from fault F19.  $\delta^{13}\text{C}_{\text{CO}_2}$  is lighter at greater distances from the fault (Fig. 9). Using a simple isotopic fractionation is difficult to explain this phenomenon (Horita, 2001; Strapoć and Schimmelmann, 2006), indicating a situation of multi-source  $\text{CO}_2$ . Coal-generated  $\text{CO}_2$

in the process of metamorphism, and  $\text{CO}_2$  derived from thermo-catalytic transformation of kerogen or soluble organic matter in coals are recognizable by  $^{13}\text{C}$  depleted isotopic signatures (Clayton, 1998), with increasing distance from F19 fault, the volume of inorganic  $\text{CO}_2$  decreases and organic  $\text{CO}_2$  increases due to longer migration distance. Two secondary causes of the deviation in carbon isotope are also proposed: 1) a finite reservoir effect accompanying the precipitation of carbonates: since carbonates are enriched in  $^{13}\text{C}$  at temperatures less than  $200^\circ\text{C}$ , their precipitation will cause the residual  $\text{CO}_2$  to become depleted in  $^{13}\text{C}$ ; and 2) coal seam's preferential adsorption to  $^{13}\text{C}_{\text{CO}_2}$  and easier desorption and migration with regard to  $^{12}\text{C}_{\text{CO}_2}$  may result in a migration of organic-origin  $\text{CO}_2$  featured with relatively light carbon isotope.

Determination of mineral content during exploration drilling demonstrates that carbonate mineral accounts for 0.2–9.6%. Carbonate contents are calculated according to the given formula (2). Higher carbonate mineral content is closer to the F19 fault, as shown in Fig. 10. Carbonate mineral, consisting primarily of calcite and siderite, is distributed in pore and crack in the Haishiwan No. 2 coal seam. The

**Table 3**

Composition of natural gas and the No. 2 coal seam samples determined from boreholes in the Haishiwan coalfield. Measured gas contents in the mine are greater than the boreholes due to the sampling process. However, the gas contents measured through the borehole may suggest the relative distribution of gasses in the coalfield.

Boreholes	Gas concentration (%)		Gas content (m <sup>3</sup> /t)		Carbonate content (%)	R <sub>o</sub> (%)	δ <sup>13</sup> C <sub>CO<sub>2</sub></sub> (‰, PDB)
	CO <sub>2</sub>	CH <sub>4</sub>	CO <sub>2</sub>	CH <sub>4</sub>			
1002	74.25	0.48	6.5	0.05	3.4	0.79	-3.66
801	43.56	1.20	0.85	0.01			
802	89.65	6.26	7.78	0.51		0.69	-0.35
803	71.98	18.58	5.16	1.32	2.7	0.83	-11.69
804	88.84	6.00	9.65	0.79	3.9	0.90	
Y45	90.89	8.96	10.0	1.00			
706	90.67	3.76	9.82	0.42	6.2	0.95	
704	79.26	7.32	7.05	0.69	6.6	0.87	
703	50.69	34.95	4.25	2.93	3.7	0.90	
705	43.01	36.25	2.00	1.96	5.2	0.92	
602	47.43	11.58	2.60	0.74	2.6	0.86	
Y49	18.71	68.79	0.30	1.24			
1401	15.47	67.12	0.82	3.82	1.6	0.96	-13.9
504	63.7	21.66	5.16	1.76	9.6	1.04	
Y33	46.59	39.12	4.10	3.99	1.3	0.95	
404	72.04	9.06	8.86	1.30	2.0	0.99	
306	82.38	2.02	7.58	0.17	6.6	1.03	
305	58.13	16.92	5.68	1.73	5.1	1.03	
304	71.58	16.14	8.24	2.02	7.0	0.97	
Y48	18.97	52.61	1.41	4.16		0.95	-14.72
302	34.26	21.36	1.31	1.15	0.2	0.89	
Y38	66.33	23.52	6.87	3.13	1.6	0.93	
Y31	55.85	25.52	7.21	3.41			-3.79
202	78.48	12.56	4.96	1.06	2.1	1.03	
Y46	23.18	64.44	0.86	2.20	0.7	0.93	-20.0
001	49.51	39.58	3.9	3.36	3.9	1.06	
Y37	23.12	60.48	2.48	6.22	0.6	0.96	

direction of carbonate distribution is consistent with CO<sub>2</sub> influx and migration. The antigenic minerals, such as dawsonite, siderite, ankerite, kaolinite, calcite, and quartz, were determined from experimental and geological studies (Watson et al., 2004; Xu et al., 2005; Worden, 2006; Liu et al., 2006; Gaus, 2010). The <sup>13</sup>C content for calcite and siderite in the second coal seam of the Yaojie No. 3 coal mine are -3.19‰ to +3.11‰ and -1.96‰ to +2.66‰(Tao, 1993), respectively, consistent with the <sup>13</sup>C content for the inorganic CO<sub>2</sub> in the coalfield (Fig. 4). The values for δ<sup>13</sup>C and δ<sup>18</sup>O and development of calcite could be eventually derived from CO<sub>2</sub> dissolution and precipitation (Li et al., 1992; Tao, 1993). Carbonate can be used as a tracer mineral of inorganic CO<sub>2</sub> migration by indicating water existence, pH value, pressure, temperature, and the original mineral (Hellevan et al., 2005; Fischer et al., 2006). The distribution of

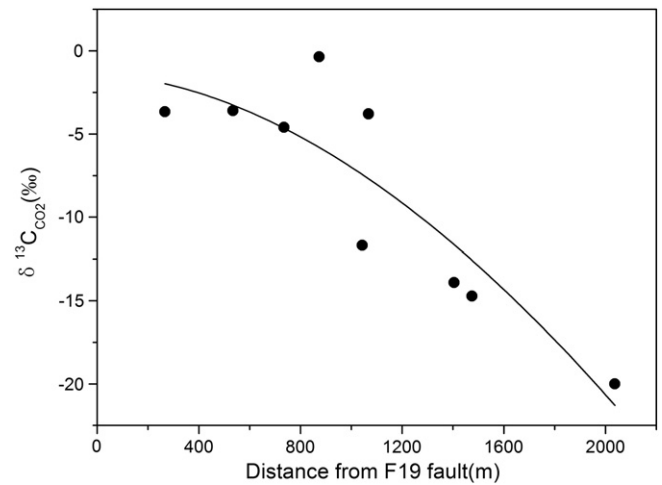


**Fig. 9.** Decreases in the CO<sub>2</sub> carbon isotope ratio as the distance from F19 increases.

carbonate in the Haishiwan minefield illustrates that CO<sub>2</sub> could alter carbonate within the range of the F19 fault.

$$\text{Carbonate content}(\%) = \frac{\text{Carbonate}}{\text{Organic maceral} + \text{Mineral impurities}} \quad (2)$$

A series of physical and chemical effects occurred after active CO<sub>2</sub> gas was injected into the coal seam, and controlled CO<sub>2</sub> migration and reservoir formation.

- (i) The injection of a higher adsorbing gas, such as CO<sub>2</sub>, would be preferentially sorbed and displace CH<sub>4</sub> from coal;
- (ii) The <sup>13</sup>CO<sub>2</sub> adsorption on coal and organic CO<sub>2</sub> migration preferentially leads to slight changes in the CO<sub>2</sub> carbon isotope in the migration direction;
- (iii) The CO<sub>2</sub> migration distance is limited to the coal seam during geological time.

The solution and adsorption of CO<sub>2</sub> in the coal seams results in a significant expansion effect of coal, such that the permeability of coal decreased (Mazumder and Wolf, 2008), which hinders CO<sub>2</sub> flow to the coal bed (Hildenbrand and Krooss, 2003). Experimental results have demonstrated when permeability is low than flow is nearly impossible even at high pressure. Thus, diffusion is the main form of transport under this condition.

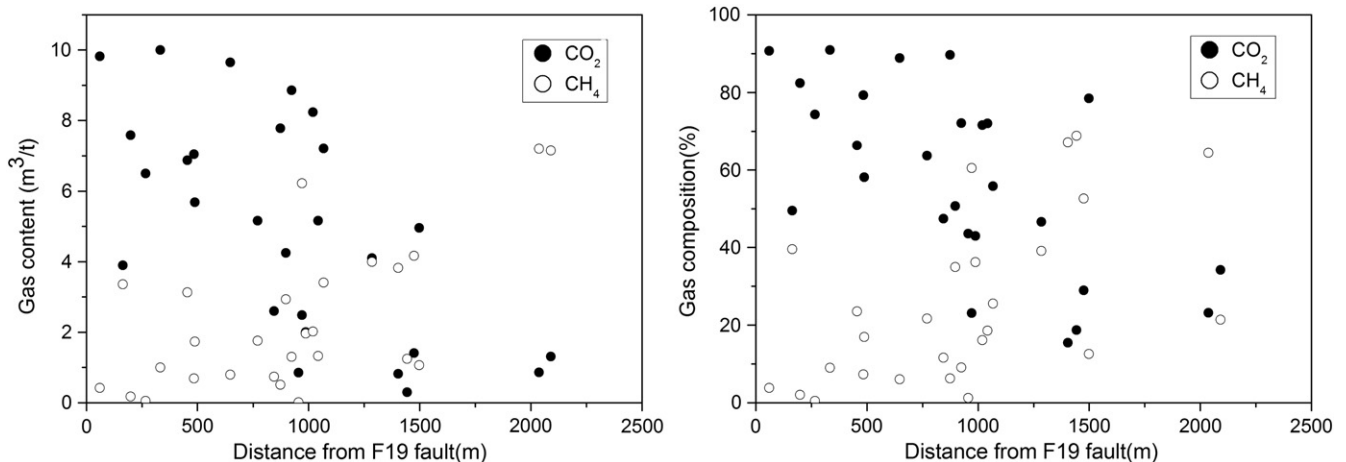


**Fig. 8.** Graph showing that the CO<sub>2</sub> content/concentration decreases and CH<sub>4</sub> content/concentration increases as the distance from F19 increases.

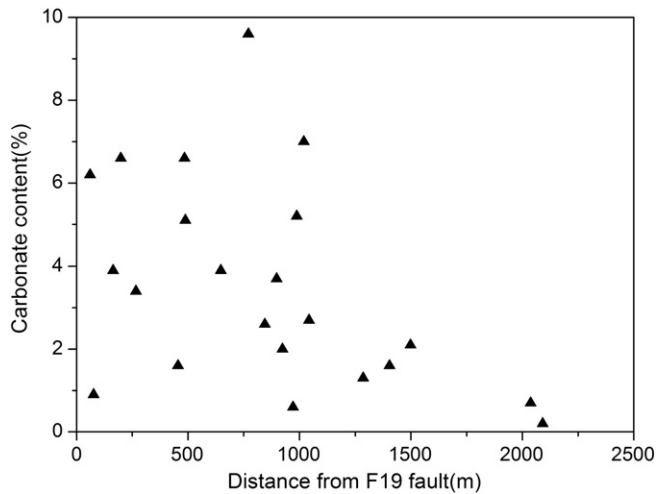


Fig. 10. Carbonate content decreases as the distance from F19 increases for the No. 2 coal seam samples.

- (iv) Under the appropriate conditions, CO<sub>2</sub> rapidly evolved into carbonate minerals in coal blocked pore fissures forming the geological storage of trapped minerals.

#### 4.4. The entrapment and accumulation of CO<sub>2</sub>

##### 4.4.1. The role of the F19 fault in CO<sub>2</sub> accumulation

The F19 fault zone is located at the eastern boundary fault of the Yaojie Coalfield and comprises of a major fault and a set branch fault that is 100 to 400 m wide extending over 17 km in length, with depth range of 300–1000 m. Currently, the characteristics of the F19 fault are normal with the Cretaceous strata exposed in hanging wall and the Jurassic exposed in footwall. The fault strikes in the SN direction and ends in the E direction. Due to strong compression, a thick coal zone of Jurassic stratum near the F19 fault was created. According to the evolutionary history of the Minhe basin, Tao et al. (1995) divided the formation of the F19 fault into five phases. The F19 fault exhibits seesaw-type tectonic movement because of a periodic variation in the tectonic stress field characteristics. Zhu and Geng (2007) proposed that at least three times the magnitude of the F19 fault tectonic movements occurred during different periods. The different move-

ment types of the F19 fault are the primary factors that control CO<sub>2</sub> generation, migration, and aggregation processes.

The F19 fault zone belongs to the third deformation style. According to Annunziatellis et al. (2008), fault zones consist of two main compartments: a central core surrounded by lateral damage zones. The fault core is the interval in which various mechanical and chemical processes have destroyed the fabric of the host rock. The system has evolved a cataclastic/gouge fault core that is relatively impermeable and a wider interval of fractures and smaller faults of damage zones provide the conduits for CO<sub>2</sub> lateral migration to coal seam. Fault development, along strike or in time, can also substantially influence secondary permeability due to changes in fracture interconnectivity and self-sealing processes.

There is no definitive evidence for the geological time scale of the CO<sub>2</sub> release in the ductile-brittle shear zone from the F19 fault. The isotopic age (K-Ar method) of chlorite thermal alteration is 15.87 Ma in the F19 fault, and the fission track age of the calcite veins in ultrabasic is 18.19 Ma ( $\pm 1.62$ ) (Tao, 1993; Wei et al., 2007). These results have demonstrated that CO<sub>2</sub> from hydrothermal activities occurred during this period. The upward movement of fluids in growth faults is proposed to be periodic. When the faults are active, fluid flow can be concentrated, but flow is restricted during inactive periods. Higher flow rates may be the result of fault-zone permeabilities and increases in fluid potential at shear stresses close to the shear strength of the rock (Hooper, 1991; Uehara and Shimamoto, 2004). Simultaneously, hydrothermal flow and precipitation may dramatically reduce existing fault-rock permeability over short time periods (Moore et al., 1994). The activities of the F19 faults in the Himalayan movement and the closed state of the NE principal stress in Quaternary are the primary factors that control CO<sub>2</sub> migration and dissipation. The CO<sub>2</sub> gas pool formation through the F19 fault zone is shown in Fig. 11.

##### 4.4.2. The entrapment system of CO<sub>2</sub> pools

During the Neogene (2.6–23.5 Ma), dynamic-thermal metamorphism of the F19 ductile-brittle shear zone proposed CO<sub>2</sub> to release from basement marble regions. In the early Neogene (15.87 Ma), there was hydrothermal vertical migration of CO<sub>2</sub> along the F19 fault. Calcite fission track ages in coal stratum (8.37–9.81 Ma) (Tao, 1993) demonstrated that during the late Neogene, there was lateral migration of CO<sub>2</sub> to the coal strata until certain pressure conditions in the F19 fault.

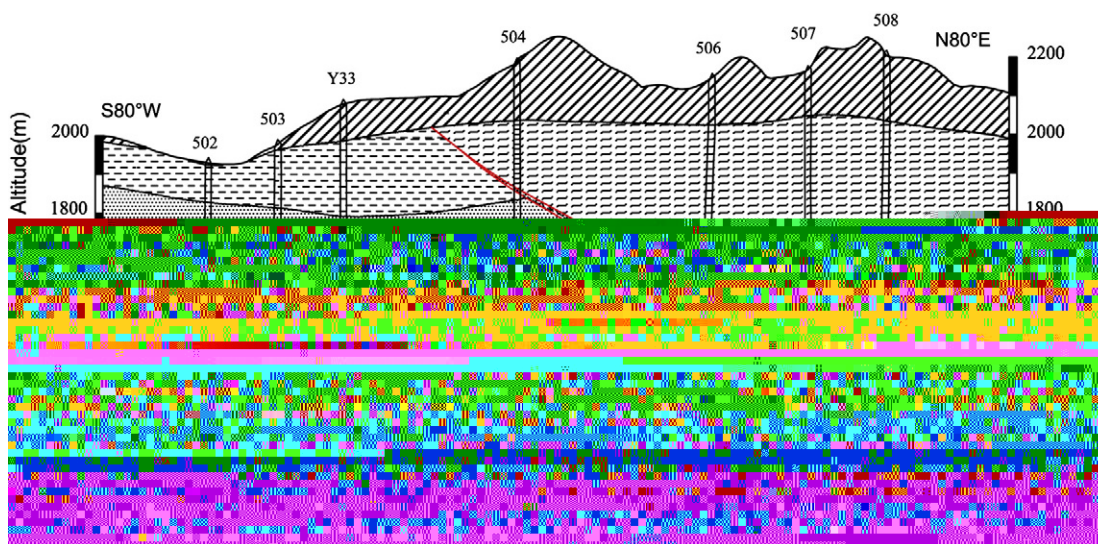


Fig. 11. Formation of the CO<sub>2</sub> gas pool through the F19 fault zone. The fault zones consist of a central core and damage zones. The fault core is impermeable, and the damage zone is the primary route of CO<sub>2</sub> migration.



The F19 fault, the roof and floor of the No. 2 coal seam constitute a CO<sub>2</sub> trap system, which seals the CO<sub>2</sub> in the coal seam effectively over geological time. The F19 fault coupled to the precipitation and cementation of carbonates that plugs fault pores results in a decrease the fracture zone permeability, which constitute a vertical trap. The mudstone permeability of the Xiangtang group is primarily in the range of  $0.03 \times 10^{-3}$  to  $0.76 \times 10^{-3} \mu\text{m}^2$ . The permeability of glutenite of the Tandonggou group is less than  $1 \times 10^{-3} \mu\text{m}^2$ , which prevents CO<sub>2</sub> dispersion. The interaction between the coal seam and the CO<sub>2</sub> at reservoir temperature, pressure, and in situ stress levels will change CO<sub>2</sub> sorption capacity, permeability, and pore structure of the coal seam to control the diffusion and flow of CO<sub>2</sub> into the coal seam.

The strong affinity between the coal seam and CO<sub>2</sub> heighten the coal sequestration capacity. However, the CO<sub>2</sub> sequestration capacity in the Yaojie coalfield remains unclear. The CO<sub>2</sub> Langmuir volumes of Haishiwan coal samples are mainly in the range of 33 to 36 m<sup>3</sup>/t. The typical drainage volume of CO<sub>2</sub> in the Haishiwan mine is not less than 45 m<sup>3</sup>/t. The phase state of CO<sub>2</sub> in the coal seam may affect the physical appearance. CO<sub>2</sub> has potential as a supercritical fluid when reservoir temperature exceeds 31.1 °C and pressure exceeds 7.38 MPa. Under typical pressures of a fresh water system, critical pressure is reached at a depth of 756 m. Indirect evidence suggests that supercritical CO<sub>2</sub> is likely to exist in the No. 2 coal seam of the Haishiwan coalfield since:

- The mining depth of the Haishiwan Mine coal is 800 m, where the coal reservoir temperature is 40 °C on average;
- The measured mixture gas pressure is not less than 7.3 MPa;
- The typical drainage volume of CO<sub>2</sub> is much larger than the expected langmuir volume;
- Strong jet phenomena with mist gas emission frequently appear during the seam drilling.

## 5. Conclusions

High CO<sub>2</sub> contents are observed in the No. 2 coal seam of the Yaojie coalfield. Gas composition reveals  $\delta^{13}\text{C}$  values for methane in the range of –32.76‰ to –44.08‰, which indicate an organic origin. However, the mainly  $\delta^{13}\text{C}_{\text{CO}_2}$  values of the gasses (–5.0‰ to +1.0‰) suggest an inorganic origin for the CO<sub>2</sub>. The <sup>3</sup>He/<sup>4</sup>He ratios of associated helium in these gasses are 0.0042–0.185 times greater than the atmospheric ratio, indicating that the helium is crust-derived.

The generation of CO<sub>2</sub> was controlled primarily by the deep F19 fault. During the late Jurassic to the early Cretaceous, dynamic-thermal metamorphism of the F19 ductile-brittle shear zone resulted in CO<sub>2</sub> release from basement carbonate regions, which are the inorganic sources of CO<sub>2</sub> in the Yaojie coalfield. The regional geological evolution and multi-periodical F19 fault movement control the formation, migration, and accumulation of CO<sub>2</sub> and result in the development of CO<sub>2</sub> gas pools in the Yaojie coalfield. The F19 fault played multiple roles in the generation, transportation, and trapping of gas during CO<sub>2</sub> formation, while the damage zone of the F19 fault is the primary route for CO<sub>2</sub> migration. The displacement of CH<sub>4</sub>, carbonation generation, and the pore structure transformation of coal occurrence due to a series of physical and chemical effects occurred after CO<sub>2</sub> flux into the coal seams.

## Acknowledgements

The authors are grateful to senior engineers Shangguan, K.F and Yuan C.L of the Yaojie Coal Electricity Group Co., Ltd. for their assistance with first-hand information of the coalfield. Funding for this research was provided by the National Foundation for the Youth of China (No. 50904068) and National Basic Research Program of China (973 Program, No. 2011CB201204). Finally we would like to thank Editor Dr. Özgen Karacan at the International Journal of Coal

Geology and reviewers of this paper for their critical and constructive review of this paper.

## References

- Annunziatellis, A., Beaubien, S.E., Bigi, S., Ciotoli, G., Coltella, M., Lombardi, S., 2008. Gas migration along fault systems and through the vadose zone in the Latera caldera (central Italy): implications for CO<sub>2</sub> geological storage. *International Journal of Greenhouse Gas Control* 2, 353–372.
- Antonellini, M., Aydin, A., Pollard, D., 1994. Microstructure of deformation bands in porous sandstones at Arches National Park, Utah. *Journal of Structural Geology* 16, 941–959.
- Ballentine, C.J., Schoell, M., Coleman, D., Cain, B.A., 2000. Magmatic CO<sub>2</sub> in natural gases in the Permian Basin, West Texas: identifying the regional source and filling history. *Journal of Geochemical Exploration* 69–70, 59–63.
- Beamish, B.B., Crosdale, P.J., 1998. Instantaneous outbursts in underground coal mines: an overview and association with coal type. *International Journal of Coal Geology* 35, 27–55.
- Cao, S.L., 1997. Structural analysis of Minhe basin. *Oil and Gas Geology* 18, 158–160.
- Clayton, J.L., 1998. Geochemistry of coalbed gas – a review. *International Journal of Coal Geology* 35, 159–173.
- Clayton, J.L., Spencer, C.W., Koncz, I., Szalay, A., 1990. Origin and migration of hydrocarbon gases and carbon dioxide, Békés Basin, Southeastern Hungary. *Organic Geochemistry* 15, 233–247.
- Evans, J.P., Foster, C.B., Goddard, J.V., 1997. Permeability of fault related rocks, and applications for hydraulic structure of fault zones. *Journal of Structural Geology* 19, 1393–1404.
- Faiz, M.M., Saghafi, A., Barclay, S.A., Stalker, L., Sherwood, N.R., Whitford, D.J., 2007. Evaluating geological sequestration of CO<sub>2</sub> in bituminous coals: the southern Sydney Basin, Australia as a natural analogue. *International Journal of Greenhouse Gas Control* 1, 223–235.
- Fischer, M., Botz, R., Schmidt, M., Rockenbauch, K., Garbe-Schönberg, D., Glodny, J., Gerling, P., Littke, R., 2006. Origins of CO<sub>2</sub> in permian carbonate reservoir rocks (Zechstein, Ca2) of the NW-German Basin (Lower Saxony). *Chemical Geology* 227, 184–213.
- GanSu Province Geology and Mining Bureau, 1989. Gansu Province of Regional Geology Memoirs. Geological publishing house, Beijing.
- Gaus, I., 2010. Role and impact of CO<sub>2</sub>-rock interactions during CO<sub>2</sub> storage in sedimentary rocks. *International Journal of Greenhouse Gas Control* 4, 73–89.
- He, S.X., Duan, J.R., Liu, J.S., Zhang, Z.R., 1996. Ductile shear zone structures and metallogeny. The Geological Publishing House, Beijing, pp. 12–62.
- Hellevar, H., Aagard, P., Oelkers, E.H., Kvamme, B., 2005. Can dawsonite permanently trap CO<sub>2</sub>? *Env. Sci. Technol.* 39 (21), 8281–8287.
- Hildenbrand, A., Krooss, B.M., 2003. CO<sub>2</sub> migration processes in argillaceous rocks: pressure-driven volume flow and diffusion. *Journal of Geochemical Exploration* 78–79, 169–172.
- Hooper, E.C.D., 1991. Fluid migration along growth faults in compacting sedimentary basins. *Journal of Petroleum Geology* 4, 161–180.
- Horita, J., 2001. Carbon isotope exchange in the system CO<sub>2</sub>–CH<sub>4</sub> at elevated temperatures. *Geochimica et Cosmochimica Acta* 65, 1907–1919.
- Hutcheon, I., Abercrombie, H.J., Krouse, H.R., 1990. Inorganic origin of carbon dioxide during low temperature thermal recovery of bitumen: chemical and isotopic evidence. *Geochimica et Cosmochimica Acta* 54, 165–171.
- Lama, R.D., Bodziony, J., 1998. Management of outburst in underground coal mines. *International Journal of Coal Geology* 35, 83–115.
- Li, Z.X., Tao, M.X., Xu, Y.C., 1992. Isotope compositions of carbonate and outburst gas in Yaojie coalfield. *Acta Sedimentologica Sinica* 10, 93–100.
- Liu, J.M., Liu, J.J., Gu, X.X., 1997. Basin fluids and their related deposits. *Acta petrologica et mineralogica* 16, 341–352.
- Liu, L., Gao, Y.Q., Qu, X.Y., Meng, Q.A., Gao, F.H., Ren, Y.G., Zhu, D.F., 2006. Petrology and carbon-oxygen isotope of inorganic CO<sub>2</sub> gas reservoir in Wuerxun depression, Hailaer basin. *Acta Petrologica Sinica* 22, 2229–2236.
- Mazumder, S., Wolf, K.H., 2008. Differential swelling and permeability change of coal in response to CO<sub>2</sub> injection for ECBM. *International Journal of Coal Geology* 74, 123–138.
- Moore, D.E., Lockner, D.A., Byerlee, J.D., 1994. Reduction of permeability in granite at elevated temperatures. *Science* 265, 1558–1561.
- O'Hara, K.D., 1994. Fluid–rock interaction in crustal shear zones: a directed dislocation approach. *Geology* 22, 843–846.
- O'Hara, K.D., William, H.B., 1989. Volume-loss model for trace-element enrichments in mylonites. *Geology* 17, 524–527.
- Pearce, J., Czernichowski-Lauriol, I., Lobardi, S., Bruned, S., Nador, A., Baker, J., Pauwels, H., Hatziyannis, G., Beaubien, S., Faber, E., 2004. A review of natural CO<sub>2</sub> accumulations in Europe as analogues for geological sequestration. In: Baines, S.J., Worden, R.H. (Eds.), *Geological Storage of Carbon Dioxide*. Geological Society, London, pp. 59–85. Special Publication 233.
- Sibson, R.H., 2000. Fluid involvement in normal faulting. *Journal of Geodynamics* 29, 469–499.
- Smith, J.W., Pallasser, R.J., 1996. Microbial origin of Australian coalbed methane. *Am. Assoc. Petrol. Geologists Bull.* 80, 807–891.
- Strapoć, D., Schimmelmann, A., 2006. Maria Mastalerz. Carbon isotopic fractionation of CH<sub>4</sub> and CO<sub>2</sub> during canister desorption of coal. *Organic Geochemistry* 37, 152–164.
- Tao, M.X., 1993. Geochemical and structural characteristics of carbon dioxide outburst in Yaojie coal mine. PhD thesis, Lanzhou institute of geology, Chinese academy of science, China.

- Tao, M.X., Xu, Y.C., Chen, F.Y., Shen, P., Sun, M.L., 1991. Helium isotope characteristics and significance of carbon dioxide gas in Yaojie coalfield. *Chinese Science Bulletin* 12, 921–923.
- Tao, M.X., Chen, F.Y., Xu, Y.C., 1995. The evolution and structural characteristics of Yaojie F19 fracture zone. *Coal Geology of China* 7, 12–16.
- Tao, S.Z., Liu, D.L., Yang, X.Y., Dai, J.X., 2000. Analysis of natural gas originating from dynamic metamorphism. *Geotectonica et Metallogenia* 24, 24–30.
- Thrasher, J., Fleet, A.J., 1995. Predicting the risk of carbon dioxide pollution in petroleum reservoirs. In: Grimalt, J.O., Dorronsoro, C. (Eds.), *Organic Geochemistry: Developments and Applications to Energy, Climate, Environment and Human History*, Proceedings of the 17th International Meeting on Organic Geochemistry, San Sebastian, Spain, pp. 1086–1088.
- Uehara, S., Shimamoto, T., 2004. Gas permeability evolution of cataclastite and fault gouge in triaxial compression and implication for changes in fault zone permeability structure through the earthquake cycle. *Tectonophysics* 378, 183–195.
- Valkiers, S., Varlam, M., Ruße, K., Berglund, M., Taylor, P., Wang, J., Milton, M., De Bi vre, P., 2007. Quantification of the degree-of-isotopic-equilibrium of carbon and oxygen isotopes in mixtures of CO<sub>2</sub> gases. *International Journal of Mass Spectrometry* 263, 195–203.
- Wang, Z.S., Zhu, D.G., 1995. A preliminary note on dynamic metamorphism duo to tectonic forces. *Journal of Geomechanics* 1, 61–65.
- Watson, M.N., Zwingmann, N., Lemon, N.M., 2004. The Ladbroke Grove-Katnook carbon dioxide natural laboratory: a recent CO<sub>2</sub> accumulation in a lithic sandstone reservoir. *Energy* 29, 1457–1466.
- Wei, P.S., Zhang, H.Q., Cheng, Q.L., Zhang, J.L., 2007. The accumulation mechanism of multi-energy mineral deposits coexisting in Minhe basin. *Petroleum Industry Press*, Beijing. pp. 27–140.
- Worden, R.H., 2006. Dawsonite cement in the Triassic Lam Formation, Shabwa Basin, Yemen: a natural analogue for a potential mineral product of subsurface CO<sub>2</sub> storage for greenhouse gas reduction. *Marine and Petroleum Geology* 23, 61–77.
- Xu, T.F., John, A.A., Karsten, P., 2005. Mineral sequestration of carbon dioxide in a sandstone-shale system. *Chemical Geology* 217, 295–318.
- Yang, X.Y., Liu, D.L., Wang, K., 1997. The component variation during mylonitization in middle to deep levels of ductile shear zones from southern part of Tancheng-Lujiang fault belt. *Geological Journal of China Universities* 3, 263–271.
- Yang, X.Y., Liu, D.L., Zhang, J.D., Cheng, Y.J., Li, Z.S., Yang, Q., 2002. Study on the element migrations and CO<sub>2</sub> releasing in the Shuangshan ductile-brittle shear zone from the South Tan-Lu fault belt. *Acta Geologica Sinica* 76, 335–346.
- Ye, X.R., Wu, M.B., Sun, M.L., 2001. Determination of the noble gas isotopic composition in rocks and minerals by mass spectrometry. *Rock and mineral analysis* 20, 174–178.
- Ye, X.R., Tao, M.X., Yu, C.A., Zhang, M.J., 2007. Helium and neon isotopic compositions in the ophiolites from the Yarlung Zangbo River, Southwestern China: the information from deep mantle. *Science in China. Series D: Earth Sciences* 50, 801–812.
- Yu, Q.X., 1992. *Mine Gas Control*. China university of mining and technology press, Xuzhou. pp. 133–138.
- Zhao, T., Zhang, Y.L., Li, Q.L., Li, Z., Qi, J.H., 2000. Lanzhou-Minhe basin tectonics and new tectonic movement related disasters discussion. *Northwestern geology* 33, 1–6.
- Zheng, Y.F., 1990. Carbon-oxygen isotopic covariation in hydrothermal calcite during degassing of CO<sub>2</sub> – a quantitative evaluation and application to the Kushikino gold mining area in Japan. *Mineral Deposita* 25, 246–250.
- Zhu, X.N., Geng, H.M., 2007. F19 fracture zone features and direction deduction to seek seam in Yaojie coalfield. *Coal Science and Technology* 35, 27–30.